

# Facile route to preparation of plate-like silver powders

Zhongchun Li<sup>1,2</sup>, Xin Zou<sup>1</sup>, Jianhua Sun<sup>1,2</sup>, Quanfa Zhou<sup>1,2</sup>

<sup>1</sup>School of Chemistry and Environment Engineering, Jiangsu University of Technology, Changzhou 213001, People's Republic of China

<sup>2</sup>Jiangsu Key Laboratory of Precious Metals Chemistry and Engineering, Changzhou 213001, People's Republic of China  
E-mail: czlize@126.com

Published in Micro & Nano Letters; Received on 25th February 2014; Revised on 20th April 2014; Accepted on 12th May 2014

Silver nanoplates with thickness of tens of nanometres and widths in the range of 5–10  $\mu\text{m}$  were successfully prepared employing a facile solution-based route based on the redox reaction between silver ions and ferrous ions. Furthermore, the influences of the mass ratio of reactants, surfactant concentration, reaction temperature and the type of surfactants on the morphologies of silver powders were carefully studied. The phase structure and morphology of silver powders are characterised by X-ray diffraction, scanning electron microscopy and high-resolution transmission electron microscopy. The mass ratio of reactants, concentration of surfactant, reaction temperature and the type of surfactants were crucial factors in determining the morphologies of the final products. The formation mechanism of silver nanoplates is preliminarily discussed.

**1. Introduction:** Metal nanostructures have attracted significant attention because of their unique physical and chemical properties [1–3]. Among various metal nanostructures, silver nanostructures are of considerable importance in catalysis, electronics, photonics and photography [4–6]. Owing to their high electrical conductivity, relatively higher melting point, high resistance to oxidation, excellent solderability, good adhesion force and reasonably price, silver nanoplates can be widely applied in various fields, such as pigments, catalytic materials, optical materials, antibacterial materials, coatings, conductive adhesives and so on [7–9]. As a conductive material, plate-like silver nanoparticles contact with each other at the boundary, which is superior to spherical particles [10]. In addition, silver nanoplates have a surface-enhanced Raman scattering effect [11]. In the past decade, much effort has been devoted to the preparation of plate-like silver powders. A variety of techniques, such as electrochemical techniques [12, 13], polymer-assisted synthesis [14, 15], polyol routes [16], the solvothermal process [17], the light induction method [18] and the wet chemical process [19], have been proved to be successful for the fabrication of plate-like silver nanostructures. However, the preparation of silver nanoplates with a well-controlled morphology and uniform size in high yield by a facile route remains a big challenge. In this Letter, a facile solution-based route for the synthesis of silver nanoplates is described. Silver nanoplates were prepared in high yield by ferrous ions reduction of silver ions with the assistance of surfactants. To determine the optimum conditions for the preparation of silver nanoplates, the experiments were carried out at various concentrations of surfactants and ferrous ions. We also investigated the effect of reaction temperature, reductant and the type of surfactants on the formation of silver nanostructures in detail. Studies revealed that plate-like silver powders with a well-defined morphology and uniform size could be obtained through this facile solution-based route. Compared with the other techniques, the remarkable advantages of our method are its simple, effective, green route and facile operation condition, which are of great value from the viewpoint of commercialisation.

## 2. Experimental

**2.1. Materials:** Silver nitrate ( $\text{AgNO}_3$ ), ammonium iron (II) sulphate hexahydrate (denoted by AISH), ferrous sulphate heptahydrate (denoted by FSH), polyvinyl pyrrolidone (PVP, K-30), cetyltrimethyl-ammonium bromide (CTAB), polyethylene

glycol 10000 (PEG10000), sodium dodecyl sulphate (SDS) and other reagents used were purchased from the Sinopharm Chemical Reagent Co. Ltd and used without further purification. The water used throughout the experiments was thrice-distilled water.

**2.2. Preparation of silver nanoplates:** Silver nanoplates were prepared through a facile solution-based route based on the redox between silver ions and ferrous ions. In a typical synthesis, 0.20 g of  $\text{AgNO}_3$  was dissolved in 15.0 ml of distilled water containing 0.04 g of PVP. At the same time, 0.40 g of AISH was dissolved in 15.0 ml of distilled water. Then ammonium iron (II) sulphate solution was dropped into the  $\text{AgNO}_3$  and PVP mixed solution at 60°C under stirring with a Teflon-coated magnetic stirring bar for 30 min in a 50 ml round flask. The final product was collected by centrifugation and washed with ethanol and water several times, and then the precipitate was dried at 60°C in vacuum condition.

**2.3. Characterisation:** The X-ray diffraction (XRD) pattern was obtained with a Bruker AXS D8 Advance diffractometer. The morphology and size of the silver powders were examined by scanning electron microscopy (SEM, HITACHI-3400s). High-resolution transmission electron microscopy (HRTEM) characterisation was performed with a FEI Tecnai G2 F30 S-TWIN field-emission transmission electron microscopy.

## 3. Results and discussion

**3.1. Morphology and structure of silver powders:** Fig. 1a shows a typical SEM image of plate-like silver powders. From Fig. 1a, we can see that the sample is composed of nanoplates with thickness of tens of nanometres and widths in the range of 5–10  $\mu\text{m}$ . A typical XRD pattern of as-prepared plate-like silver powders is shown in Fig. 1b. Five diffraction peaks are observed at  $2\theta = 38.1, 44.2, 64.5, 77.5$  and  $81.6$ , which correspond to the (111), (200), (220), (311) and (222) reflections of face-centered cubic silver with lattice constant  $a = 4.08989 \text{ \AA}$ , respectively (JCPDS No. 04-0783) [5, 20, 21]. The sharpness of the peaks implies that the sample is well crystallised and no other sign of impurities was detected. The XRD result shows that the high crystalline quality of the plate-like silver powders could be obtained through this facile route. It is worth noting that the intensity ratio between (111) and (200) diffractions ( $I_{(111)}/I_{(200)}$ ) of 17.6 for the prepared plate-like silver powders is much higher than the conventional bulk intensity ratio (the theoretical ratio is 2.5) [22]. The unusual

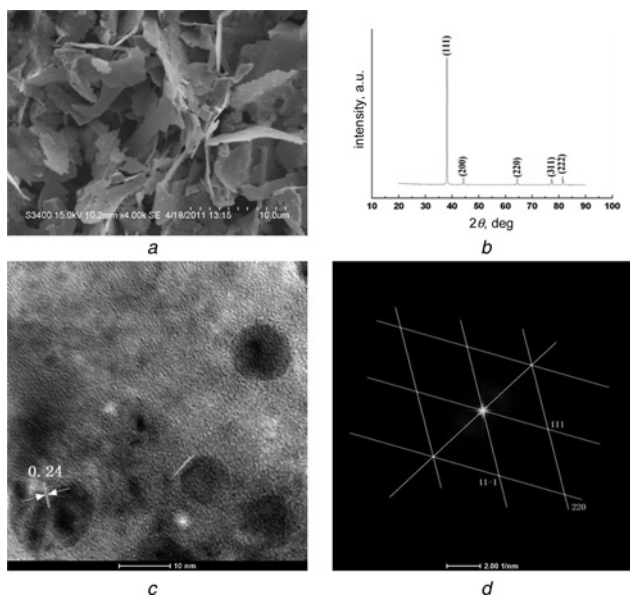


**Figure 1** SEM image of plate-like silver powders XRD pattern, HRTEM, FFT pattern  
 a SEM image of plate-like silver powders  
 b XRD pattern  
 c HRTEM  
 d FFT pattern  
 $m(\text{AgNO}_3):m(\text{AISH}) = 1:2$ ,  $m(\text{PVP}) = 0.04$  g,  $T = 60^\circ\text{C}$

intensity of the (111) diffraction peak indicates that the faces of silver nanoplates are primarily composed of (111) planes as confirmed by HRTEM measurement. For further insight into the crystal structure of the silver nanoplate, structural analyses of the silver nanoplate were performed by HRTEM and fast Fourier transform (FFT). Fig. 1c shows a typical HRTEM image of the silver nanoplate. The fringe spacing is 0.24 nm, which is close to the (111) lattice spacing of face-centered cubic silver [23]. Fig. 1d is the corresponding FFT pattern of the HRTEM image, which further confirms that the as-prepared silver nanoplate is a single crystal structure [24].

**3.2. Effect of the mass ratio of  $\text{AgNO}_3/\text{AISH}$  on the morphologies of silver powders:** In our synthesis, the concentration of  $\text{AgNO}_3$  was fixed, and the AISH and/or PVP concentration was changed to obtain plate-like silver powders. Fig. 2 shows the SEM images of silver powders prepared at different mass ratios of  $\text{AgNO}_3/\text{AISH}$ . At the mass ratio between  $\text{AgNO}_3$  and AISH of 1:1, plate-like silver powders with a well-defined morphology were obtained (Fig. 2a). When the mass of  $\text{AgNO}_3/\text{AISH}$  was decreased to 2:5 or 1:3, the products were dominated by silver nanoplates. However, the size of the silver nanoplates was not uniform (Figs. 2b and c). The morphology transformed to the mixture of nanorods, nanoplates and nanoparticles as shown in Fig. 2d at the lower mass of  $\text{AgNO}_3/\text{AISH}$  (2:7). The above results indicate that a suitable AISH concentration is needed to obtain silver nanoplates with a well-defined morphology and uniform size.

**3.3. Effect of PVP concentration on the morphologies of silver powders:** Fig. 3 represents the SEM images of silver powders prepared with different PVP mass at the constant mass ratio of  $\text{AgNO}_3/\text{AISH}$  (1:2). When the experiment was conducted without PVP, lamellar nanostructures accompanied with nanoparticles and block structures could be found in Fig. 3a. When the mass of PVP was increased to 0.02 g, major products were the silver nanoplates, accompanied with slight nanoparticles on the surface of the silver nanoplates (Fig. 3b). At the mass of 0.04 g, well-defined silver nanoplates were achieved with thickness of

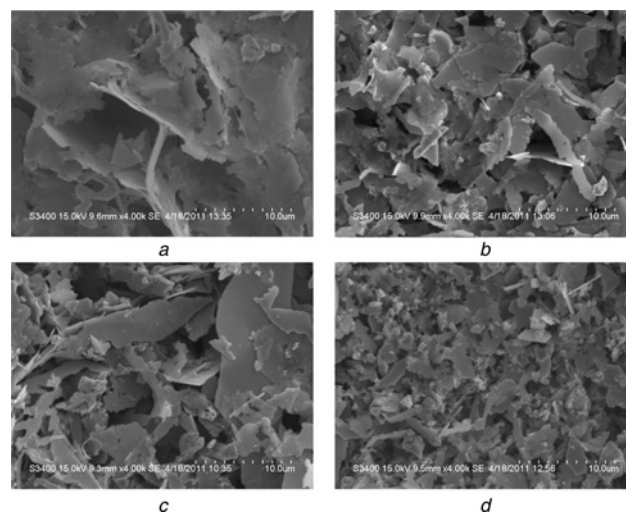


**Figure 2** SEM images of silver powders prepared at different ratios of  $\text{AgNO}_3/\text{AISH}$   
 $m(\text{AgNO}_3):m(\text{AISH})$   
 a 1:1  
 b 2:5  
 c 1:3  
 d 2:7

tens of nanometres and widths in the range of 5–10  $\mu\text{m}$  (Fig. 3c). When the mass of PVP was increased to the higher value (0.08 g), plate-like nanostructures could also be obtained. However, other morphologies of particles were found in the sample and the size of plate-like nanostructures was not uniform, as depicted in Fig. 3d. It is obvious that the addition of different amounts of PVP could tune the morphology of the final product. The PVP concentration available in the reaction system is very important to the synthesis of well-defined silver nanoplates.

**3.4. Effect of reaction temperature on the morphologies of silver powders:** For further insight into the influences of reaction temperature on the morphologies of silver powders, the experiments were performed at different temperatures with the mass ratio between  $\text{AgNO}_3$  and AISH of 1:2. Figs. 4a and b

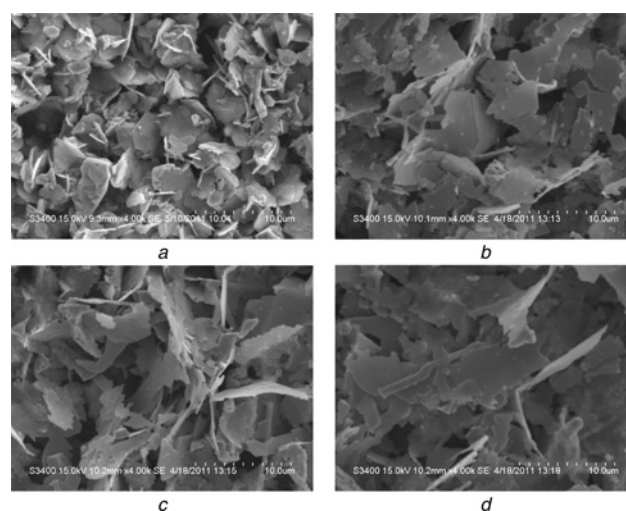


**Figure 3** SEM images of silver powders prepared at different PVP mass  
 $m(\text{PVP})/\text{g}$   
 a 0  
 b 0.02  
 c 0.04  
 d 0.08

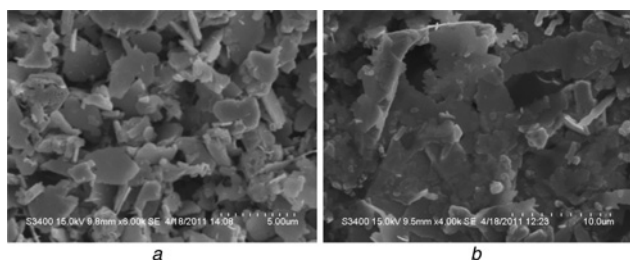


**Figure 4** SEM images of silver powders prepared at different reaction temperatures

Reaction temperature/°C

a 40

b 80

show the SEM images of samples prepared at 40 and 80°C, respectively. The silver powders were composed of lamellar and block structures when the reaction was carried out at 40°C (Fig. 4a). When the reaction temperature was increased to 80°C, significant change in the morphology of the sample occurred. Only a few silver nanoplates were found in the SEM image (Fig. 4b). The above experimental results show that the reaction temperature significantly affected the morphologies of the final products. Only when a suitable reaction temperature was chosen could well-defined silver nanoplates could be produced.

**3.5. Effect of surfactants on the morphologies of silver powders:** Comparative experiments were conducted to investigate the effect of surfactants on the morphologies of silver powders. Three different types of surfactants including CTAB, PEG10000 and SDS were applied to substitute the PVP under the same experimental conditions of Fig. 1. Representative SEM images of the products prepared with various surfactants are shown in Fig. 5. As shown in Fig. 5a, triangular nanoplates, polyhedrons and small particles were obtained when cationic surfactant CTAB was used in the synthesis of silver powders. Interestingly, well-defined silver nanoplates were achieved when PEG10000 was applied in the synthesis process (Fig. 5b). A possible reason is that PVP and PEG10000 belong to the same type of surfactants (non-ionic surfactant). As depicted in Fig. 5c, only a few amounts of plate-like structures were obtained if PVP was substituted by anionic surfactant SDS in the synthesis process. Therefore, the

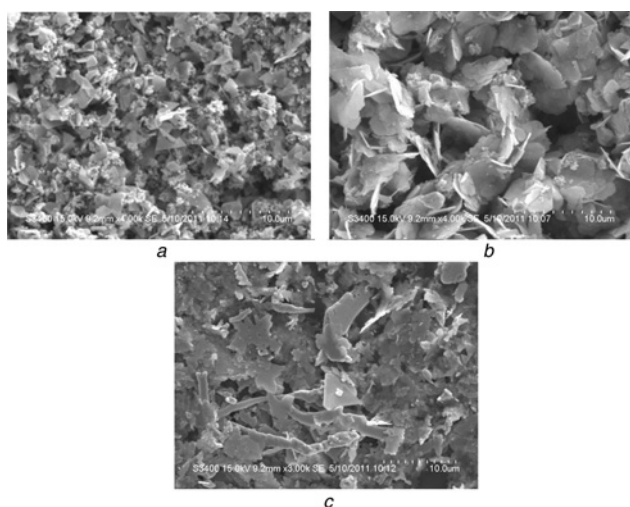


**Figure 5** SEM images of silver powders prepared with different surfactants

a CTAB

b PEG10000

c SDS

type of surfactants has an important effect on the morphologies of silver powders.

**3.6. Effect of reductant on the morphologies of silver powders:** In our synthesis, silver powders were prepared by the reaction as follows.



From (1), we can know that  $\text{Fe}^{2+}$  was used as the reductant in the synthesis reaction. To investigate the influence of reductant on the morphologies of silver powders, FSH was used as the reductant and other experimental conditions were kept the same as those of Fig. 1. Fig. 6 depicts the SEM images of silver powders prepared with different surfactants when FSH was used as the reductant. From Fig. 6a, we can see that silver nanoplates and small particles were obtained when PVP was used as the surfactant. Significant change in morphology occurred when CTAB was applied in the synthesis process. The sample was composed of polyhedrons and small particles (Fig. 6b). As depicted in Figs. 6c and d, the major products were silver nanoplates with different sizes when PEG10000 and SDS were employed, respectively. It is reasonable to believe that surfactant and reductant have an important effect on the morphologies of silver powders.

**3.7. Possible formation mechanism of silver nanoplates:** As is known, reaction conditions affect the morphology and size of the samples. To investigate the nucleation and growth process of silver nanoplates, a series of experiments have been carried out. From the above results, it can be observed that the morphologies are greatly dependent on the experimental conditions, such as the mass ratio of  $\text{AgNO}_3/\text{AISH}$ , PVP concentration, the type of surfactants and the reaction temperature. To gain control over the synthesis, it is necessary to understand the mechanism by which silver nanoplates are formed. A general order of the surface energies for different faces of the face-centered cubic metals may hold,  $\gamma\{111\} < \gamma\{100\} < \gamma\{110\}$ . That means more energy is released by adding a silver atom to the  $\{100\}$  faces or  $\{110\}$  faces than to  $\{111\}$  faces during crystal growth [25]. These faces, which have a higher surface energy compared to the others, have a great tendency to bind to surfactant such as PVP. PVP may act

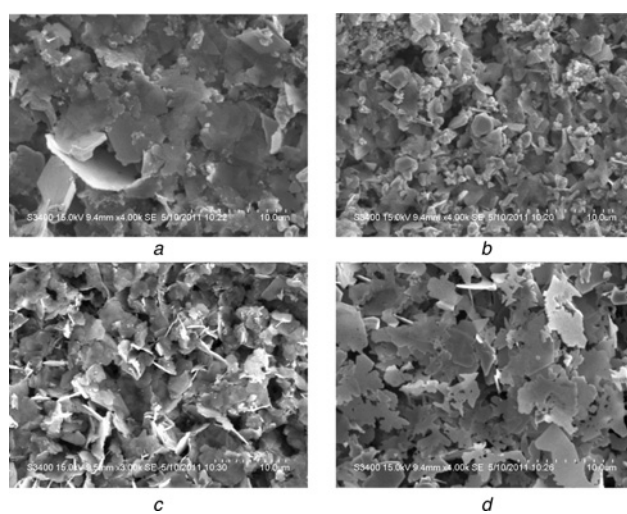


**Figure 6** SEM images of silver powders prepared with different surfactants

a PVP

b CTAB

c PEG10000

d SDS

as capping agents in the crystal growth process. Ag clusters may be covered with PVP molecules which lead to the growth of plate-like nanostructures.

**4. Conclusion:** In summary, plate-like silver powders with thickness of tens of nanometres and widths in the range of 5–10  $\mu\text{m}$  were prepared employing a facile solution-based route based on the redox reaction between  $\text{Ag}^+$  and  $\text{Fe}^{2+}$ . The mass ratio of  $\text{AgNO}_3/\text{AISH}$ , the concentration of surfactant and the type of surfactants have significant influences on the morphologies of silver powders. The obtained plate-like silver powders may find potential applications in catalysis, conductive pastes or microelectronic devices.

**5. Acknowledgments:** This work is supported by the National Science and Technology Support Program (2014BAC03B06), the National Natural Scientific Foundation of China (21373103) and the University Natural Scientific Foundation of Jiangsu Province (11KJB150003).

## 6 References

- [1] Xia Y., Xiong Y., Lim B., *ET AL.*: ‘Shape-controlled synthesis of metal nanocrystals: simple chemistry meets complex physics?’, *Angew. Chem. Int. Ed.*, 2009, **48**, (1), pp. 60–103
- [2] Siril P.F., Ramos L., Beaumier P., *ET AL.*: ‘Synthesis of ultrathin hexagonal palladium nanosheets’, *Chem. Mater.*, 2009, **21**, (21), pp. 5170–5175
- [3] Sun Y., Xia Y.: ‘Shape-controlled synthesis of gold and silver nanoparticles’, *Science*, 2002, **298**, (5601), pp. 2176–2179
- [4] Wiley B., Sun Y., Mayers B., *ET AL.*: ‘Shape-controlled synthesis of metal nanostructures: the case of silver’, *Chem. Eur. J.*, 2005, **11**, (2), pp. 454–464
- [5] Li Z., Gu A., Guan M., *ET AL.*: ‘Large-scale synthesis of silver nanowires and platinum nanotubes’, *Colloid Polym. Sci.*, 2010, **288**, (10–11), pp. 1185–1191
- [6] Li Z.C., Zhou Q.F., He X.H., *ET AL.*: ‘Synthesis of silver nanocubes and nanorods through sodium-bromide-assisted polyol route’, *Micro Nano Lett.*, 2011, **6**, (4), pp. 261–264
- [7] Gentry S.T., Fredericks S.J., Krchnavek R.: ‘Controlled particle growth of silver sols through the use of hydroquinone as a selective reducing agent’, *Langmuir*, 2009, **25**, (5), pp. 2613–2621
- [8] Deckert-Gaudig T., Erver F., Deckert V.: ‘Transparent silver microcrystals: synthesis and application for nanoscale analysis’, *Langmuir*, 2009, **25**, (11), pp. 6032–6034
- [9] Wu S.P.: ‘Preparation of micron size flake silver powders for conductive thick films’, *J. Mater. Sci., Mater. Electron.*, 2007, **18**, (4), pp. 447–452
- [10] Liguó Y., Yanhua Z.: ‘Preparation of nano-silver flake by chemical reduction method’, *Rare Met. Mater. Eng.*, 2010, **39**, (3), pp. 401–404
- [11] Jin-long T., Bin T., Shu-ping X., *ET AL.*: ‘Comparison of surface-enhanced Raman scattering spectra of two kinds of silver nanoplate films’, *Chem. Res. Chin. Univ.*, 2012, **28**, (3), pp. 488–492
- [12] Liu G., Duan G., Jia L., *ET AL.*: ‘Fabrication of self-standing silver nanoplate arrays by seed-decorated electrochemical route and their structure-induced properties’, *J. Nanomater.*, 2013, **2013**, pp. 1–7
- [13] Liu G., Cai W., Kong L., *ET AL.*: ‘Vertically cross-linking silver nanoplate arrays with controllable density based on seed-assisted electrochemical growth and their structurally enhanced SERS activity’, *J. Mater. Chem.*, 2010, **20**, (4), pp. 767–772
- [14] Trandafilović L.V., Luyt A.S., Bibić N., *ET AL.*: ‘Formation of nanoplate silver particles in the presence of polyampholyte copolymer’, *Colloid Surf. A*, 2012, **414**, pp. 17–25
- [15] Abdul Kareem T., Anu Kaliani A.: ‘Synthesis and thermal study of octahedral silver nano-plates in polyvinyl alcohol (PVA)’, *Arab. J. Chem.*, 2011, **4**, pp. 325–331
- [16] Darmanin T., Nativo P., Gilliland D., *ET AL.*: ‘Microwave-assisted synthesis of silver nanoprisms/nanoplates using a “modified polyol process”’, *Colloid Surf. A*, 2012, **395**, pp. 145–151
- [17] He X., Zhao X., Li Y., *ET AL.*: ‘Shape-controlled synthesis for silver: triangular/hexagonal nanoplates, chain-like nanoplate assemblies, and nanobelts’, *J. Mater. Res.*, 2009, **24**, (7), pp. 2200–2209
- [18] Zhou Q., Xu Z.: ‘The preparation of nano-scale plate silver powders by visible light induction method’, *J. Mater. Sci.*, 2004, **39**, (7), pp. 2487–2491
- [19] Lee B.-H., Hsu M.-S., Hsu Y.-C., *ET AL.*: ‘A facile method to obtain highly stable silver nanoplate colloids with desired surface plasmon resonance wavelengths’, *J. Phys. Chem. C*, 2010, **114**, (14), pp. 6222–6227
- [20] Li Z.C., Shang T.M., Zhou Q.F., *ET AL.*: ‘Sodium chloride assisted synthesis of silver nanowires’, *Micro Nano Lett.*, 2011, **6**, (2), pp. 90–93
- [21] Li Z.C., Zhou Q.F., Sun J.H.: ‘Potassium iodide-assisted polyol route synthesis of monodisperse silver nanospheres’, *Micro Nano Lett.*, 2010, **5**, (3), pp. 175–177
- [22] Jiu J., Murai K., Kim D., *ET AL.*: ‘Preparation of Ag nanorods with high yield by polyol process’, *Mater. Chem. Phys.*, 2009, **114**, (1), pp. 333–338
- [23] Zhang D., Qi L., Yang J., *ET AL.*: ‘Wet chemical synthesis of silver nanowire thin films at ambient temperature’, *Chem. Mater.*, 2004, **16**, (5), pp. 872–876
- [24] Im S.H., Lee Y.T., Wiley B., *ET AL.*: ‘Large-scale synthesis of silver nanocubes: the role of HCl in promoting cube perfection and monodispersity’, *Angew. Chem. Int. Ed.*, 2005, **44**, (14), pp. 2154–2157
- [25] Lu L., Kobayashi A., Tawa K., *ET AL.*: ‘Silver nanoplates with special shapes: controlled synthesis and their surface plasmon resonance and surface-enhanced Raman scattering properties’, *Chem. Mater.*, 2006, **18**, (20), pp. 4894–4901